Polymer 51 (2010) 1837–1844

Contents lists available at ScienceDirect

Polymer

journal homepage: www.elsevier.com/locate/polymer

Microbeam X-ray diffraction of non-banded polymer spherulites of it-polystyrene and it-poly(butene-1)

Hiroshi Kajioka, Shigeru Yoshimoto, Ratan C. Gosh, Ken Taguchi, Shinpei Tanaka, Akihiko Toda*

Graduate School of Integrated Arts and Sciences, Hiroshima University, Higashi-Hiroshima 739-8521, Japan

ARTICLE INFO

Article history:
Received 27 October 2009
Received in revised form
15 February 2010
Accepted 15 February 2010
Available online 21 February 2010

Keywords:
Non-banded spherulite
it-Polystyrene
Microbeam X-ray

ABSTRACT

The orientation of lamellar crystals in non-banded spherulites of it-polystyrene and it-poly(butene-1) was investigated by microbeam X-ray diffraction. The two-dimensional intensity map of diffraction enables us to examine the local orientation of lamellar crystallites in the non-banded spherulites. The obtained results indicated the re-orientation of crystallites in non-banded spherulites and confirmed our previous observation on the anisotropic birefringence of a group of crystal stacks by polarizing optical microscopy.

1. Introduction

Crystallization of polymers from the melt evolves a structure called spherulite formed by chain-folded lamellar crystals with radiating and space filling branches [1–3]. The structure of polymer spherulites is classified into two types; those are with and without periodic extinction pattern under polarizing optical microscopy (POM), as seen in Fig. 1. So-called banded spherulites are with the periodic pattern due to lamellar twisting along the radial axis. As discussed in detail by Lotz and Cheng [4], the lamellar twist is supposed to be due to unbalanced surface stresses on the upper and lower lamellar surfaces caused by the steric hindrance among chain foldings. For the surface stresses in the direction choosing handedness, lamellar crystals are supposed to be spontaneously twisted in one of the handedness, i.e., right or left, in the banded spherulites.

The formation of periodic banding requires not only the lamellar twist but also the coherence of twist along the tangential direction in the spherulites. For polymers forming banded spherulites, therefore, the disappearance of periodic banding can be caused by the loss of coherence. On the other hand, there is another type of polymers which do not show any banding under any crystallization conditions. Isotactic polystyrene (itPS) and poly(butene-1) (itPB1) in the form II are the cases. Even for those intrinsically non-banded spherulites, there should also be unbalanced surface stresses by chain foldings, though the stresses will not be in the direction choosing the handedness of the twist. In non-banded spherulites of this type, the crystallites are supposed to be twisted back and forth in a random manner.

Banded spherulites are characterized quite clearly by the band spacing of the periodic extinction pattern, and numerous studies have been done on the structure of banded polymer spherulites in terms of the band spacing [1–3]. On the other hand, non-banded spherulites have not been well characterized in a quantitative manner in preceding studies, and not so many studies have been made on the structure. We have recently suggested that the structure of non-banded spherulites can be characterized by the patchy pattern, which consists of thin and long threads along the radial axis, as seen in Fig. 1b [5]. For the quantitative examination of the patchy pattern in non-banded spherulites, we have defined the auto-correlation function of the POM image along the radial direction, and experimentally examined the dependence of the correlation function on the distance along the radial direction. The dependence could be well approximated by a single exponential decay, which suggested the random re-orientation of lamellar crystals. The inverse of the slope of the decay defines the persistence length, which corresponds to the mean size of the patchy pattern along the radial direction of spherulites.

By examining the microscopic structure of lamellar crystals at the growth front, it has been confirmed that the width of lamellar

* Corresponding author. Tel.: +81 82 424 6558; fax: +81 82 424 0757.
E-mail address: atoda@hiroshima-u.ac.jp (A. Toda).

0032-3861/$ – see front matter © 2010 Elsevier Ltd. All rights reserved.
doi:10.1016/j.polymer.2010.02.025

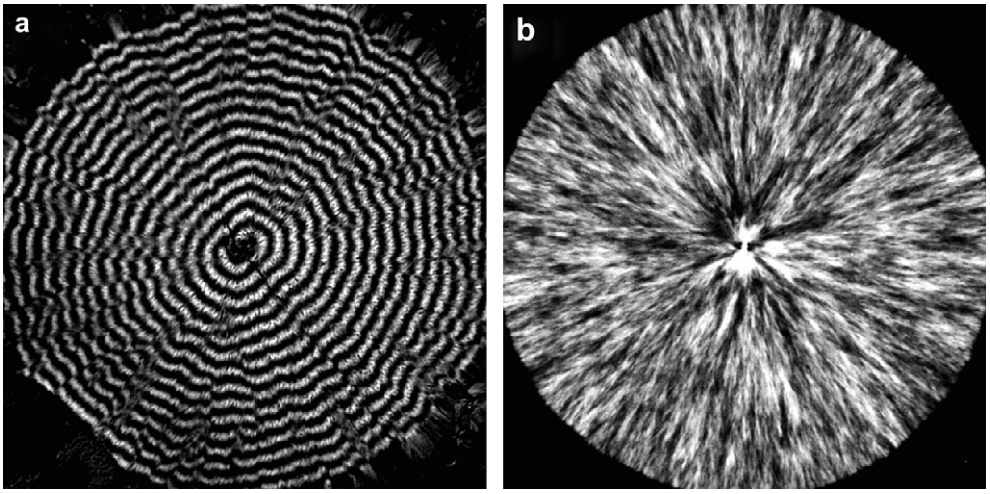

Fig. 1. POM images of (a) a banded spherulite of poly(vinylidene fluoride) and (b) a non-banded spherulite of it-poly(butene-1). The images were obtained by the sum of two images of the same area differing in the angle of polarizer by 45° while keeping the condition of cross-nicols. The image size is 200 μm × 200 μm.

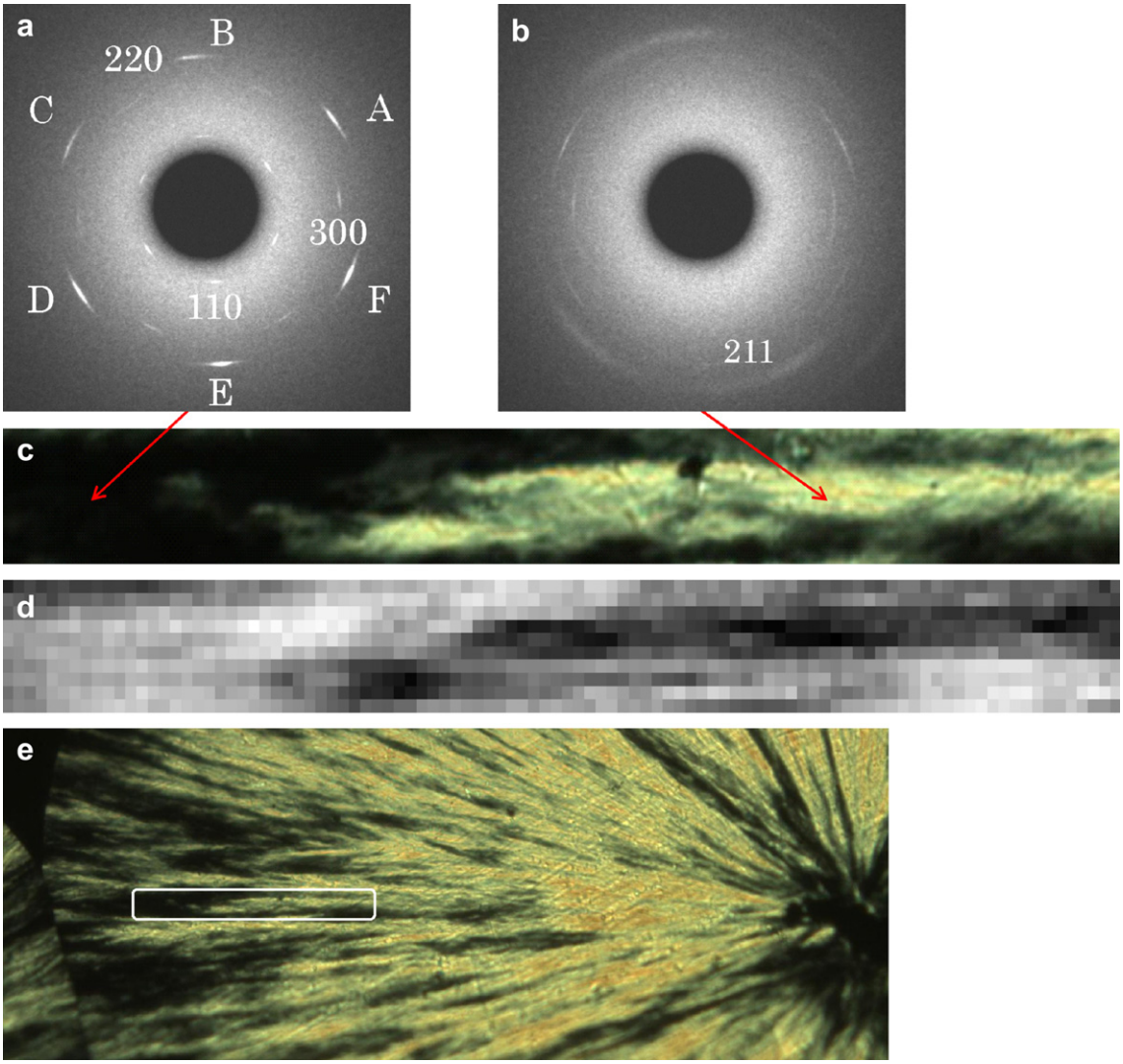

Fig. 2. Diffraction patterns, (a) and (b), from the points indicated by the arrows in (c), which is a 200 μm × 20 μm × POM image of a part of itPS spherulite shown in the POM image of (e), as indicated by a box with white lines. In (d), two-dimensional map (100 × 10 points) of the sum of the intensity of the 220 reflections, I_{220}, is shown for the same area as in (c).

crystals is in proportion to the persistence length. Similar proportionality has also been confirmed for the banded spherulites of polyethylene [6,7] and poly(vinylidene fluoride) [8] between the band spacing and the lamellar width. The proportional relationship clearly indicates a quite simple view that the structure of polymer spherulites at larger scale is determined by the size of the building blocks. It is noted that the relationship can be expected for both of the cases of discontinuous re-orientation on the occasion of branching and continuous re-orientation along the lamellar crystals. So, by those experimental results, we cannot suggest either of those two possible mechanisms of discontinuous or continuous re-orientation.

In the previous work on non-banded spherulites [5], the correlation of lamellar orientation along the radial axis has been examined by means of polarizing optical microscopy (POM) displaying the pattern of birefringence in spherulites. The POM image only represents the change in the crystal orientation averaged over lamellar stacks, and the direct and microscopic confirmation of the re-orientation of lamellar crystals in non-banded spherulites has not yet been done experimentally.

In banded spherulites, the lamellar twisting has been directly confirmed by wide angle X-ray diffraction with the scanning of collimated beam, the size of which is in the order of μm or below [9–12]. By analyzing the change in diffraction pattern for the two-dimensional map of microbeam X-ray diffraction, it is further possible to follow the crystal orientation in the sample. In a recent work, Nozue et al. [11] could identify the left- and right-handed twists along the growth direction of crystallites in a banded spherulite of poly(ε-caprolactone).

The two-dimensional intensity map of microbeam X-ray diffraction can also be utilized to identify the direction of re-orientation of crystallites in non-banded spherulites. In the present paper, in order to confirm the re-orientation of lamellar crystals in non-banded spherulites, we examine the spherulites of itPS and itPB1 formed in the form II by means of microbeam X-ray diffraction which is available at a synchrotron radiation facility. The microbeam X-ray is focused to a sub-micron scale at the sample position with a Fresnel zone plate and scanned over the sample to directly see the change of crystal orientation in the form of diffraction patterns.

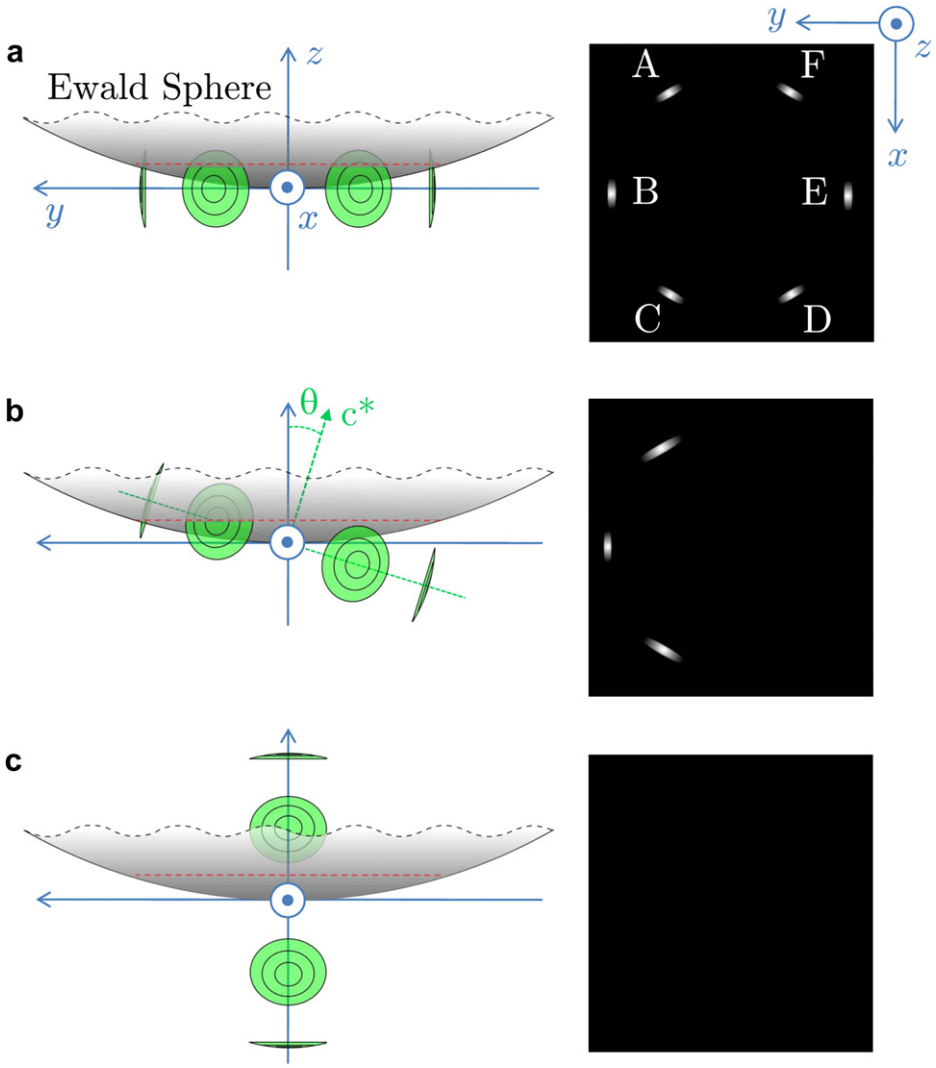

Fig. 3. Reciprocal space and the expected 220 diffraction pattern for the re-orientation of lamellar crystals with the rotation axis (*x*-axis) in the radial direction of spherulite [10,11]. The target patterns represent angular spread of the 220 reciprocal lattices. The diffraction condition is satisfied for the intersections with the Ewald sphere. The diffractions, A–F, correspond to those in Fig. 2a.

2. Experimental

Isotactic polystyrene, itPS, (M_w = 556,000, M_w/M_n = 1.9) was purchased from Polymer Laboratories Ltd. Isotactic poly(butene-1), itPB1, (M_w = 674,000, M_w/M_n = 4.7) was kindly supplied by Sun Allomer Ltd. These polymers form non-banded and large spherulites (≥300 μm).

Thin films (*ca.* < 10 μm of itPS and ~3 μm of itPB1) were prepared by pressing polymer powder between aluminum foils in the molten state. The films were then melted, crystallized isothermally at 197 °C for itPS and at 101.5 °C for itPB1, and cooled down to room temperature. The aluminum foils were peeled off subsequently for the examination of X-ray diffraction. When itPB1 is crystallized from the melt, a metastable form, Form II (tetragonal) [13], is obtained. Form II is then transformed to the stable form, Form I, (trigonal: $a = 1.77$ nm, $c = 0.65$ nm referred to the hexagonal lattice) [14,15] at room temperature. The crystallized samples of itPB1 were kept more than a few days at room temperature and the transformed samples were examined.

The microbeam wide angle X-ray diffraction was carried out at the BL47XU beamline of the SPring-8 synchrotron radiation facility in Japan. The wavelength of the beam was 0.155 nm and the focal spot size of 0.6 × 0.7 μm^2 was generated by Fresnel zone plate optics [16]. The diffraction pattern was intensified with an image intensifier having Be window of 4-inch in diameter (V7739, Hamamatsu Photonics). The image was recorded with a CCD (C4742-98-24A, Hamamatsu Photonics). The diffraction patterns were taken at the step of 2 μm along the radial and tangential directions of the spherulites. The exposure time was 1 s and the interval between data acquisitions was 10 s. The intensity profile was calibrated for dark current and polarization. The images of the scanned area were taken before and after scanning by a movable optical microscope equipped on the beamline.

3. Results and discussion

Fig. 2a and b are the diffraction patterns from the points indicated by the arrows in Fig. 2c, which is a POM image of a part of an itPS spherulite in Fig. 2e. The X-ray diffraction patterns were taken in the area at the interval of 2 μm in the horizontal and vertical directions. The scanned area (100 × 10 points) marked by the white box in Fig. 2e is far from the center of the spherulite, and hence the growth direction of the crystallites in the area is nearly parallel to the horizontal direction.

In Fig. 2a taken from the dark area of the POM image in Fig. 2c, the bright hk0 reflections, 110, 300, 220, of the trigonal crystal of itPS (a = 2.19 nm, c = 0.665 nm referred to the hexagonal lattice) [17] are observed. The result suggests that, in this area of the spherulite, the direction of the c-axis is nearly parallel to that of the incident beam, in accordance with the dark POM image indicating the optical axis pointing to the incident ray. In Fig. 2a, it is also seen that the direction of the pair of 300 reflections corresponds to the radial (horizontal) direction of the spherulite in Fig. 2e. This relationship is expected from the growth direction of crystallites normal to the {100} plane in itPS spherulites. On the other hand, in Fig. 2b taken from the bright area of the POM image, the intensities of the hk0 reflections are weak and the 211 reflections appear. In this area, both of the X-ray and POM results indicate the tilting of the c-axis in terms of the incident beam.

Fig. 3 shows the schematic relationship between the reciprocal space with the rotation of crystal orientation and the diffraction pattern [10,11]. In Fig. 3, the reciprocal-lattice points are drawn as circular targets representing the broadening of the lattices due to small size of polymer crystallites and the distribution of orientation. Experimentally, the broadening is suggested by e.g., the appearance of all 6 reflections of the 220 reflections in Fig. 2a. In Fig. 3, it is seen that the tilting of the c-axis results in the asymmetric pattern of the 220 reflections. As discussed below, by utilizing the asymmetric change of the intensities, we can directly identify the crystal orientation.

For an angular spread of the reciprocal-lattice points approximated by an isotropic Gaussian type [10], the integrated intensity of all the 220 reflections is calculated in Fig. 4a as a function of the angle, θ, between the sample plane normal which is in the direction of the incident beam and the lamellar plane normal which is tilted with the rotation axis in the direction of the radial axis of the spherulite. In the calculation, the full width of half height (FWHH) of the spread of the reciprocal-lattice points was set at 20° in order to account for the manner of appearance of the reflections with the present sample, as discussed below. This width reflects both of the size of crystallites and of the angular distribution of crystal orientation. In terms of the size of crystallites, it is known that the lamellar thickness is ~3 nm when crystallized at 190 °C [18]. Owing to the broadening of the reciprocal-lattice points due to the size effect, FWHH is estimated to be ≃9° for the 220 reflections. The larger angle of FWHH (~20°) indicates that the contribution of the distribution of crystal orientation is important to account for the spread of the reciprocal-lattice points.

In Fig. 4a, the POM intensity, I_{POM}, is also plotted against the angle, θ, which corresponds to the angle between the optical axis

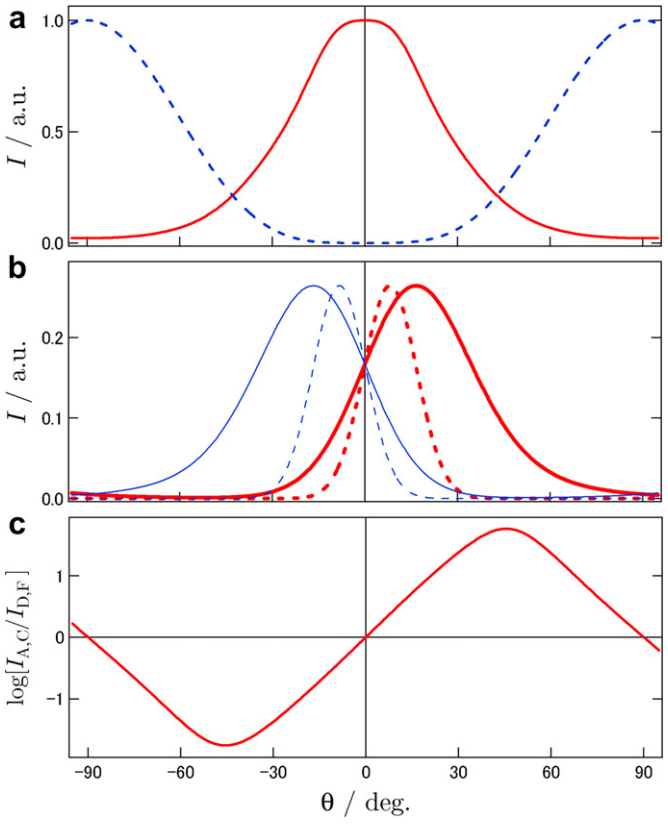

Fig. 4. Intensity profile plotted against the angle, θ, between the sample plane normal and the lamellar plane normal which is tilted with the rotation axis in the direction of the radial axis of spherulite: (a) the sum of the intensity of all the 220 reflections, I_{220}, (solid line) and the brightness of POM image (broken line), (b) the 220 reflection at the azimuthal angles of 30° and 150° from the horizontal position of the diffraction pattern, $I_{A,C}$ (thick solid line), I_B at 90° (thick broken line), $I_{D,F}$ at 210° and 330° (thin solid line), and I_E at 270° (thin broken line), and (c) the logarithm of the ratio, log [$I_{A,C}/I_{D,F}$]. FWHH of an isotropic Gaussian type for the spread of reciprocal-lattice points is set at 20°.

and the propagation direction of incident ray. Here, the POM intensity was calculated from the following equation [5]:

$$I_{\mathrm{POM}} = I(\mu,\theta) + I\left(\mu+\frac{\pi}{4},\theta\right) \sim I_0\left(\frac{\pi t}{\lambda}\right)^2 |n_c - n_o|^2 \sin^4\theta \qquad (1)$$

where I_0 represents the intensity of incident light, t is the sample thickness, λ is the wavelength of incident light, and n_c and n_o are the refractive index along the optical axis of the crystal and that of ordinary ray, respectively. The angle, μ, represents the azimuthal angle between the axis of polarizer and the projection of the optical axis of the crystal onto the plane made by the axes of polarizer and analyzer. The above equation is for an optically uniaxial crystal, such as the trigonal itPS crystal and the trigonal (Form I) and tetragonal (Form II) crystal modifications of itPB1. The intensity, I_{POM}, is the sum of two images of the same area differing in the angle of polarizer by $\pi/4$ rad while keeping the condition of cross-nicols. The equation indicates that the sum of the images becomes independent of the azimuthal angle, μ. The typical examples of the summed image are shown in Fig. 1 of banded and non-banded spherulites without the Maltese cross.

Fig. 4a suggests the reversed relationship between the brightness of POM image and the X-ray intensity of all the 220 reflections. In order to experimentally examine the change in lamellar orientation in a spherulite, microbeam X-ray was scanned at a step of 2 μm in the radial and tangential directions of the spherulite to get the two-dimensional intensity map. For each cell examined, the intensities of all 220 reflections were summed up and mapped in gray scale in Fig. 2d. The POM image of Fig. 2c and the X-ray intensity map of Fig. 2d confirm the reversed relationship as expected from Fig. 4a. This correlation confirms the estimation method of crystal orientation by POM in our previous work [5], even though the POM image represents the crystal orientation averaged over lamellar stacks in polymer spherulites.

Let us next examine the change in crystal orientation in the two-dimensional X-ray diffraction map. For non-banded spherulites, we expect the crystallites twisting back and forth in a random manner. As shown in Fig. 4a, the intensity of POM image does not distinguish the back and forth twist, e.g., $\theta = -90^\circ \rightarrow 0^\circ \rightarrow -90^\circ$, from the twist in one direction, e.g., $\theta = -90^\circ \rightarrow 0^\circ \rightarrow +90^\circ$. Both cases produce the changes from bright ($\theta = -90^\circ$) to dark ($\theta = 0^\circ$) and then again to bright ($\theta = -90^\circ$ or $+90^\circ$).

In terms of the 220 diffractions, by examining the change in each of the diffractions, not in the total sum, I_{220}, we can distinguish the manner of the twist. It means that the diffraction intensities of A, B and C and those of D, E and F in Fig. 2a behave in a different way for the back and forth twist and for the twist in one direction. In Fig. 4b, the intensity, $I_{A,C}$, corresponds to that of the diffraction peaks at A and C in Fig. 2a, I_B to B, $I_{D,F}$ to D and F, and I_E to E, respectively. As seen in Fig. 4b, since the intensities become maximum at different tilting angle, θ, the re-direction of crystals in this angular range can be discriminated by examining the changes in the intensities. The logarithm of the ratio, log $[I_{A,C}/I_{D,F}]$, in Fig. 4c indicates a direct correspondence between the ratio and the rotation angle, θ, in the angular range of $-45^\circ < \theta < 45^\circ$, where the intensities of the 220 reflections are appreciable.

Fig. 5 shows the experimental intensity map of each diffraction peak at the position of A–F in the same area as those in Fig. 2c and d; some of the diffraction patterns are shown in Fig. 6. For the calculation of the peak intensities, the background was subtracted

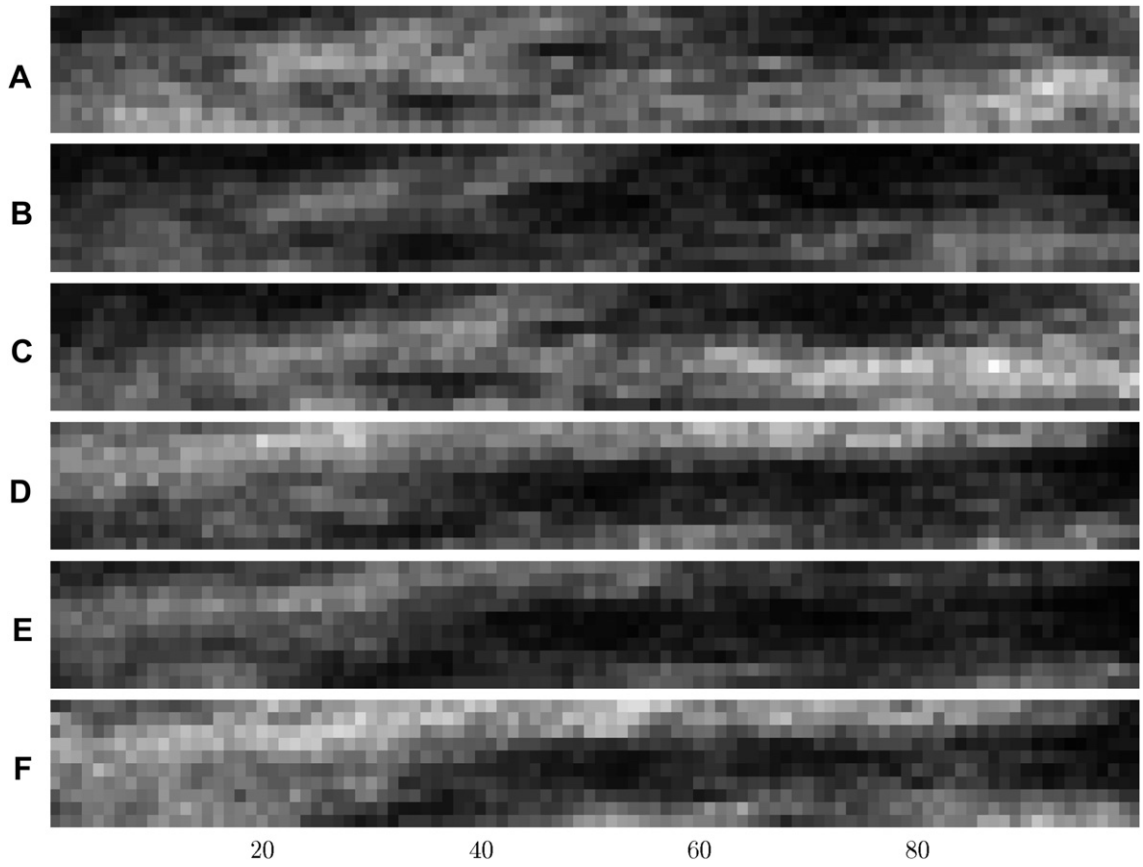

Fig. 5. Two-dimensional maps of the intensity of the 220 reflections at A, B, C, D, E and F in Fig. 2a for the same area of 100 × 10 points as in Fig. 2c and d.

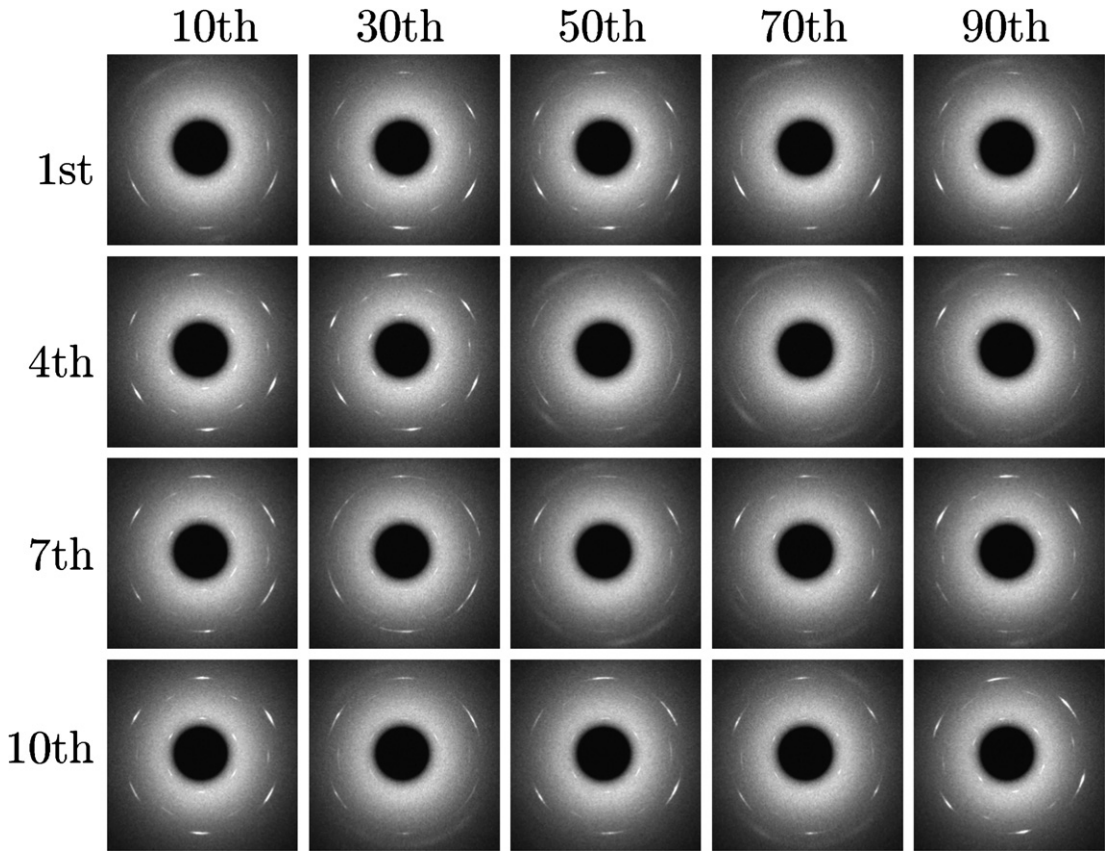

Fig. 6. Diffraction patterns at the positions with corresponding column and row numbers in Fig. 5.

and the intensities were integrated over ±30° around the peak centers. By comparing the maps in Fig. 5, it is seen that the changes are the types of the back and forth re-direction of crystallites. For example, the intensities in the upper part of Fig. 5A and C become maximum at the position (the 44th column) different from the two maximum positions of $I_{D,\,F}$ at the 24th and 64th columns. The sum of the intensities, $I_A + I_C$ and $I_D + I_F$, of the 1st row in Fig. 7a directly shows the manner of re-direction. In the 1st row at around the 20th column, $I_A + I_C$ is remarkably weaker than $I_D + I_F$, indicating $\theta < 0°$. With shifting the position to the right columns, the intensities become comparable at the 44th column ($\theta \simeq 0°$), and then again become weaker ($\theta < 0°$) with further shift to the right. The changes can also be confirmed in the diffraction patterns shown in Fig. 6: at the 30th and 70th columns, the hk0 intensities (including $I_{A,\,B,\,C}$) in the upper half are weaker than those (including $I_{D,\,E,\,F}$) in the lower half, while the intensities are comparable at the 50th.

The manner of re-direction can be understood more easily by the logarithmic plots of the ratio, log $[(I_A + I_C)/(I_D + I_F)]$, shown in Fig. 8 for the 1st, 4th, 7th and 10th rows. In comparison with the calculated change shown in Fig. 4c, the zigzag changes in the ratio of Fig. 8 confirm the manner of the back and forth re-direction of crystallites in those areas. It is noted that, in the left part at around the 43rd column of the 4th row, even though the ratio seems to be continuously changing around unity, there should have been a large angle re-orientation ($\theta° \sim 0° \rightarrow \theta° \sim 90°$ in Fig. 4c) indicated by the discontinuous changes in the POM image seen in Fig. 2c and the total sum of the diffraction intensities, I_{220}, in Figs. 2d and 7b. We suppose that the competition of growth domains will probably be the cause of this large angle re-orientation. In this way, though the changes may not be those of single domain of crystallites, the result clearly indicates the ability of the direct identification of crystal orientation by microbeam X-ray diffraction. In principle, it is possible to do the

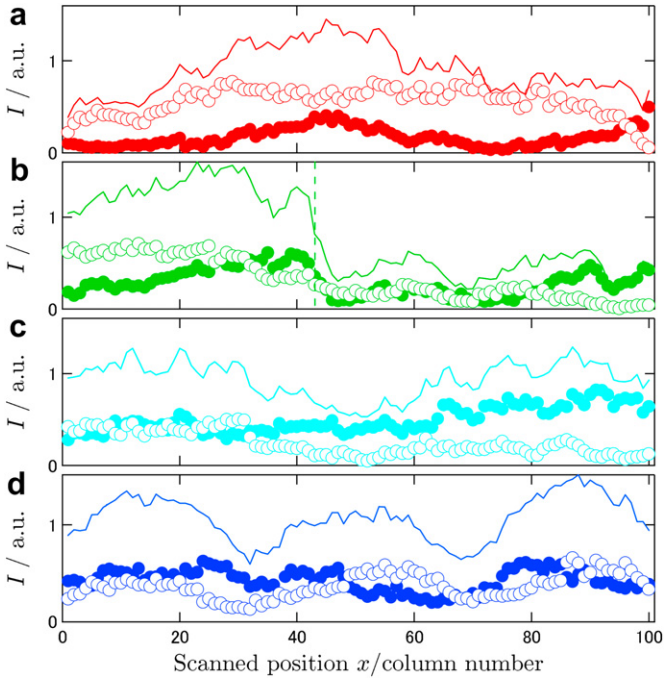

Fig. 7. Intensities of $I_A + I_C$ (●) and $I_D + I_F$ (○) at (a) the uppermost (1st), (b) 4th, (c) 7th, and (d) the bottom (10th) rows of Fig. 5, respectively, plotted against the column number of the scanned position, x. The lines indicate the total sum, I_{220}. The broken vertical line in (b) indicates a sudden change in the total sum.

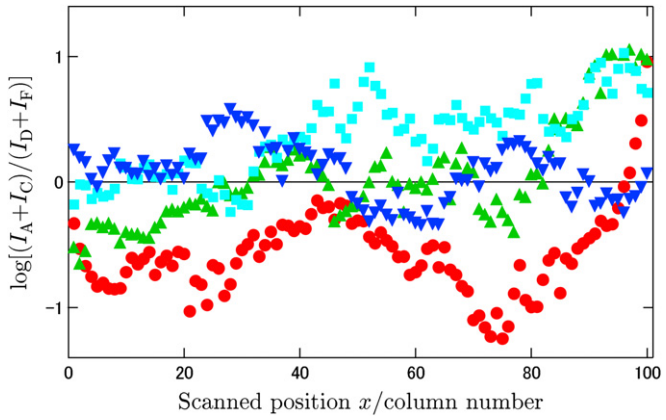

Fig. 8. Logarithm of the ratio, log $[(I_A + I_C)/(I_D + I_F)]$, for the uppermost (1st) (●), 4th (▲), 7th (■), and the bottom (10th) (▼) rows of Fig. 5 plotted against the column number of the scanned position, x.

quantitative evaluation of the rotation angle for the experimentally determined ratio in comparison with the calculated ratio in Fig. 4c, in which the FWHH of the plot was normalized by the maximum of the experimental ratio of Fig. 8. However, we suppose that the obtained ratio is influenced by isotropic reflections from unoriented crystallites probably formed as a secondary crystallization. Therefore, we have concluded that the quantitative evaluation was not meaningful for the present experimental results.

For itPB1 non-banded spherulites, due to the weak resistance against radiation and due to the solid–solid phase transition after crystallization, the detailed analysis of the two-dimensional intensity map could not be done. Fig. 9a–e of itPB1 corresponds to those in Fig. 2a–e of itPS. The reversed relationship between the brightness of POM image and the X-ray intensity of all the 110 reflections is confirmed for itPB1, too. Namely, at the cell where the c-axis is parallel to the incident beam, I_{110} is strong and I_{POM} is weak, and vice versa. This correlation seen in Fig. 9 confirms the validity of our estimation of lamellar orientation by POM in our previous work [5]. It is also noted that the diffraction pattern of the transformed form I modification shown in Fig. 9a is consistent with the [110] growth direction of the form II crystals along the radial direction in the spherulites, as reported previously [5,19].

As final remarks on the application of the present method, the followings should be noted. Firstly, in terms of the identification of crystal orientation, we can also apply POM or transmission electron microscopy (TEM) as well as microbeam X-ray. The advantage of microbeam X-ray in comparison with TEM is the applicability to thicker films of relatively bulky samples. On the other hand, the identification by POM is known to be possible in principle but not

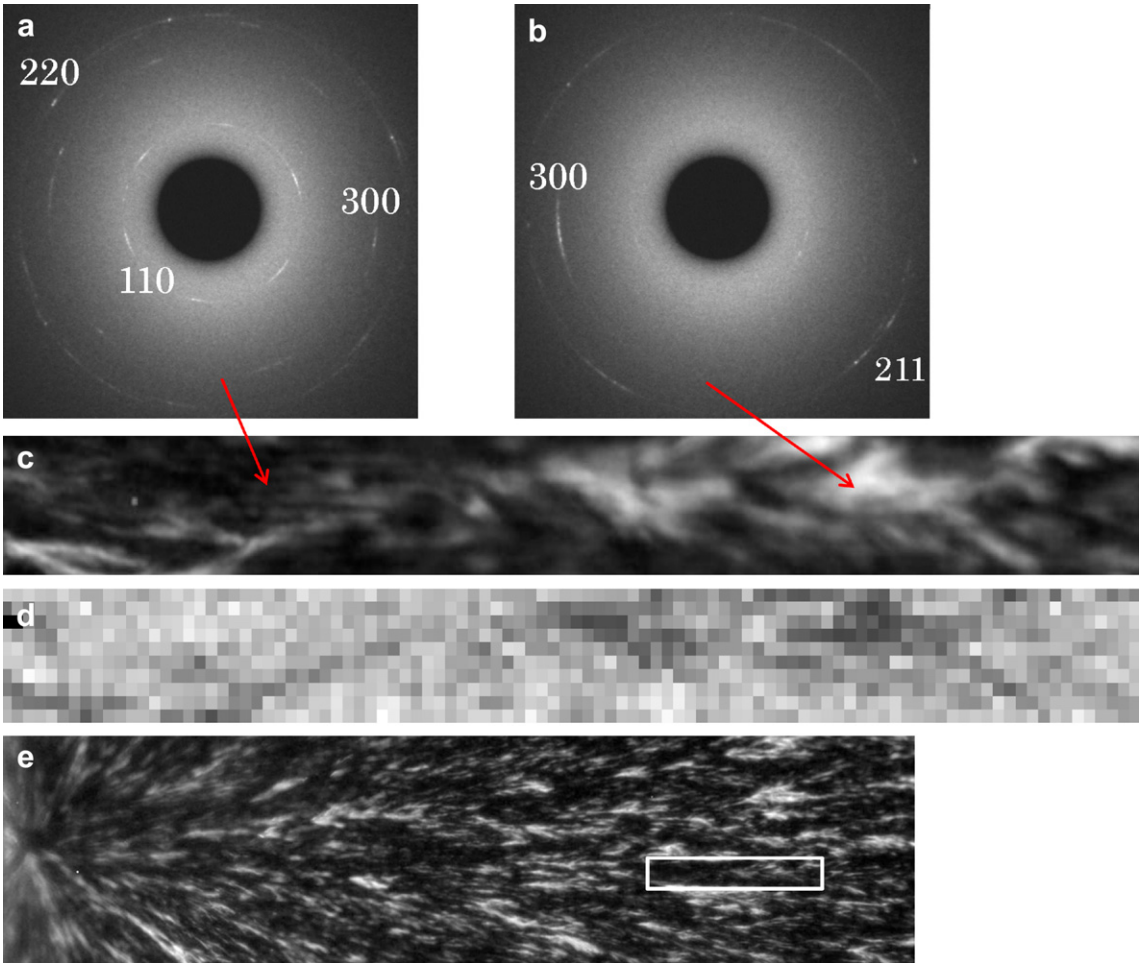

Fig. 9. Diffraction patterns, (a) and (b), from the points indicated by the arrows in (c), which is a 200 μm × 20 μm POM image of a part of itPB1 spherulite shown in the POM image of (e), as indicated by a box with white lines. In (d), two-dimensional map (100 × 10 points) of the sum of the intensity of the 110 reflections is shown for the same area as in (c).

in a straightforward way [20,21]. It is further noted that the POM image includes both of the crystal and amorphous anisotropy in the case of polymer samples, while the diffraction of microbeam X-ray comes from the crystal orientation. Therefore, the combination of POM and microbeam X-ray enables us the distinction of the amorphous anisotropy from crystal orientation. Such an attempt has been reported for oriented polymer samples by using X-ray diffraction with ordinary beam size and the birefringence of POM [22].

Secondly, it is also noted that the sample thickness is an important factor for the present method. If it is too large including a group of fibrils of lamellar crystallites in the thickness direction, then the orientation of lamellar crystals observed through the film will be random and isotropic. For the sample thinner than the lamellar width, on the other hand, the re-orientation mechanism of lamellar crystals can be influenced by the sample thickness. We suppose that the sample thickness of the present experiments, *c.a.* 10 μm for itPS and 3 μm for itPB1, is thick enough in comparison with the lamellar width, while the thickness is thin enough to observe the anisotropic orientation.

4. Conclusions

We have examined the structure of non-banded spherulites of itPS and itPB1 formed in the form II by means of microbeam X-ray diffraction. The microbeam X-ray of sub-micron size was scanned over the film at a distance of 2 μm along the radial and tangential directions of the spherulites to obtain the two-dimensional map of the diffraction patterns. The results suggested the direct confirmation of the crystal re-orientation in the non-banded spherulites in accordance with our previous results obtained by the analysis of POM images. In this way, the details of the re-orientation, such as the lamellar twisting or the random re-orientation, can be identified by examining the two-dimensional map of the microbeam X-ray diffraction patterns.

Acknowledgments

This work was partially supported by MEXT Japan, Grant-in-Aid for Scientific Research on Priority Areas, “Creation of Non-equilibrium Soft Matter Physics”. The synchrotron radiation experiments were performed at the BL47XU in the SPring-8 with the approval of Japan Synchrotron Radiation Research Institute (JASRI) (Proposal No. 2007B1667). The authors are grateful to Dr. K. Yamada (Sun Allomer Ltd.) for the kind supply of poly(butene-1). The authors are also grateful to SPring-8 at JASRI for supporting this WAXS experiments.

References

[1] Geil PH. Polymer single crystals. New York: Wiley; 1963.
[2] Magill JH. J Mater Sci 2001;36:3143.
[3] Bassett DC. J Macromol Sci 2003;B42:227.
[4] Lotz B, Cheng SZD. Polymer 2005;46:577.
[5] Kajioka H, Hikosaka M, Taguchi K, Toda A. Polymer 2008;49:1685.
[6] Toda A, Okamura M, Taguchi K, Hikosaka M, Kajioka H. Macromolecules 2008;41:2484.
[7] Toda A, Taguchi K, Kajioka H. Macromolecules 2008;41:7505.
[8] Toda A, Taguchi K, Hikosaka M, Kajioka H. Polym J 2008;40:905.
[9] Fujiwara Y. J Appl Polym Sci 1960;4:10.
[10] Nozue Y, Kurita R, Hirano S, Kawasaki N, Ueno S, Iida A, et al. Polymer 2003;44:6397.
[11] Nozue Y, Hirano S, Kurita R, Kawasaki N, Ueno S, Iida A, et al. Polymer 2004;45:8299.
[12] Tanaka T, Fujita M, Takeuchi A, Suzuki Y, Uesugi K, Doi Y, et al. Polymer 2005;46:5673.
[13] Turner-Jones A. J Polym Sci B 1963;1:455.
[14] Natta G, Corradini P, Bassi IW. Nuovo Cim Suppl 1960;15:52.
[15] Boor Jr J, Mitchell JC. J Polym Sci A 1963;1:59.
[16] Suzuki Y, Takeuchi A, Takano H, Ohigashi T, Takenaka H. Jpn J Appl Phys 2001;40:1508.
[17] Natta G, Corradini P, Bassi IW. Nuovo Cim Suppl 1960;15:68.
[18] Fukao K, Miyamoto Y. Polymer 1993;34:238.
[19] Yee RY, Stein RS. J Polym Sci A 1970;8:1661.
[20] Keller A. J Polym Sci 1959;39:151.
[21] Singfield KL, Hobbs JK, Keller A. J Cryst Growth 1998;183:683.
[22] Hoshino S, Powers J, LeGrand DG, Kawai H, Stein RS. J Polym Sci 1962;58:185.